Finite-Volume Schemes on the Cubed-Sphere

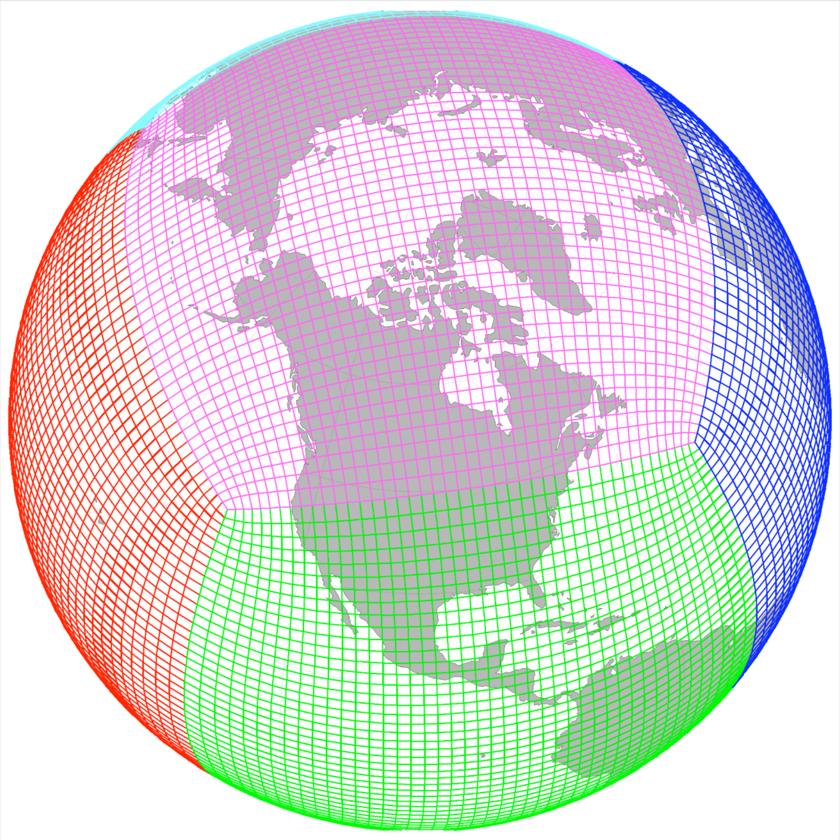

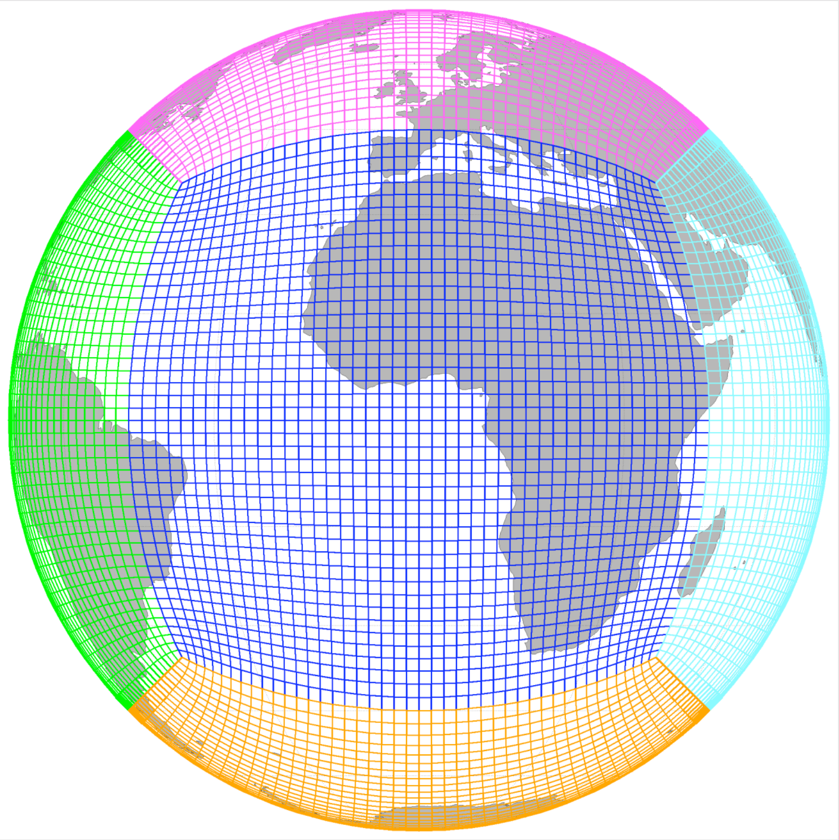

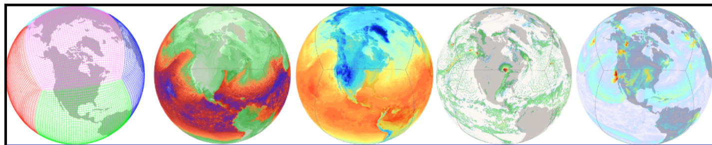

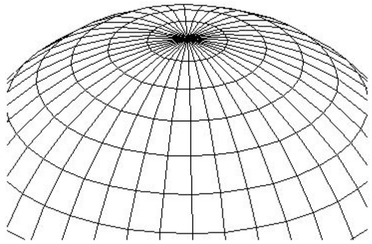

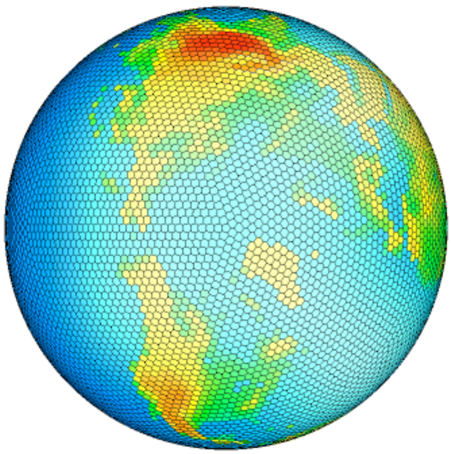

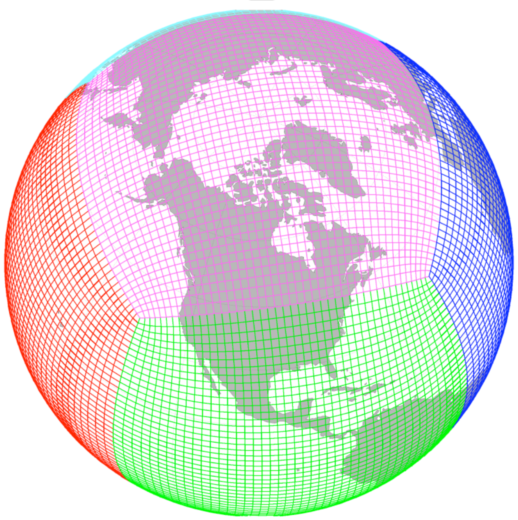

Global Spherical Grid Options

Motivated by Parallel Scalability

- Latitude-longitude grids
  - Logically rectangular spherical grid
  - Suffers from the convergence of meridians at the poles
    - Zonal grid spacing converges at the poles ***(over-sampling)***
- Icosahedral Geodesic Grids ***(icosahedron - triangles)***
  - Isotropic (near-uniform)
  - Hexagonal/Triangular shaped cells
  - Non-orthogonal
  - Eliminates over-sampling near the spherical poles
  - Suitable for massively parallel implementation
- The Cubed-Sphere ***(hexahedron - quadrilaterals)***
  - Quasi-Uniform mapping of the cube to a sphere
    - ***Gnomonic (Sadourny, 1972)***
    - ***Conformal (Rancic & Purser, 1996)***
    - ***Elliptic Solvers / Spring Dynamics***
  - Quadrilateral shaped cells
  - Ideal for 2D X-Y Domain Decomposition ***(parallelism)***
  - Suitable for adaptive mesh refinement

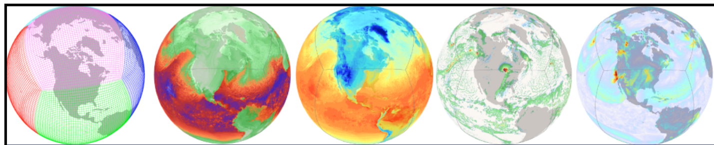

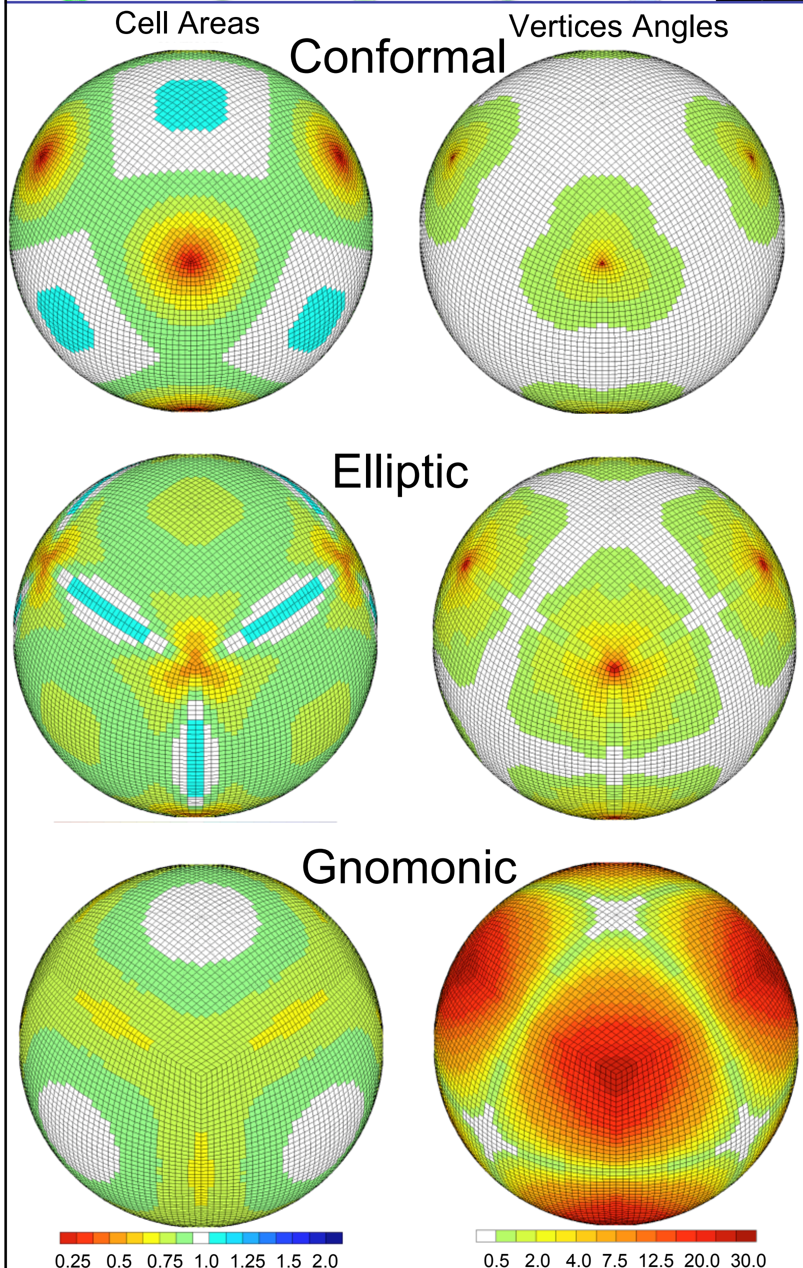

Cubed-Sphere Grid Options

Uniformity / Orthogonality

- The <u>Conformal</u> Cubed-Sphere
  - *Rancic, Purser, Mesinger, 1996*
  - *McGregor, 1996*
  - 8 pole-like singularities (clustering of grid cells, CFL problems)
  - Orthogonal grid / Continuous across edges
- Grids modified by <u>Elliptic Solvers</u> / <u>Spring Dynamics</u>
  - *Putman and Lin, 2007*
  - Better uniformity near 8-corners
  - Quasi-Orthogonal
- The <u>Gnomonic</u> Cubed-Sphere
  - *Sadourny. 1972*
  - *McGregor, 1996*
  - Quasi-Uniform
  - Non-orthogonal / discontinuities across face edges
  - Coordinate lines are arcs of great circles

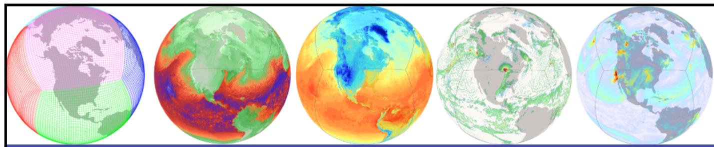

Finite-Volume Advection

Multi-Dimensional Flux-Form Transport

(Lin and Rood, 1996)

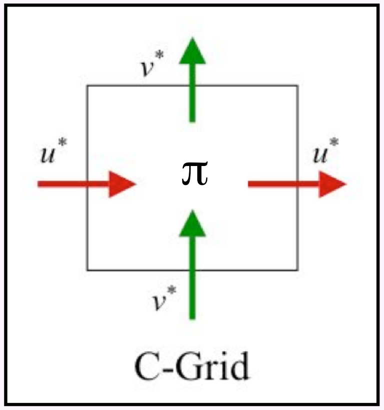

Directionally split

$$\tilde{\pi}^{n+1} = \tilde{\pi}^n + F\left[u^*, \Delta t, (\tilde{\pi})^y\right] + G\left[v^*, \Delta t, (\tilde{\pi})^x\right]$$

1D flux-form operators

$$F(u^*, \Delta t, \tilde{\pi}) = -\frac{\Delta t}{\mathcal{A}}\,\delta_x\left[u^*\,\Delta y\,\pi^*(u^*, \Delta t, \tilde{\pi})\right]$$

$$G(v^*, \Delta t, \tilde{\pi}) = -\frac{\Delta t}{\mathcal{A}}\,\delta_y\left[v^*\,\Delta x\,\pi^*(v^*, \Delta t, \tilde{\pi})\right]$$

Cross-stream inner-operators

$$()^x \equiv ()^n + \frac{1}{2} f\left[u^*, \Delta t, ()^n\right]$$

$$()^y \equiv ()^n + \frac{1}{2} g\left[v^*, \Delta t, ()^n\right]$$

- Eulerian
- Stable for CFL < 1
- Identical to original schemes developed for cartesian Lat-Lon grid
- Can be directly adopted on Conformal grid

c90
Conformal

Day-12
Cosine Bell
Error

Alpha=45º

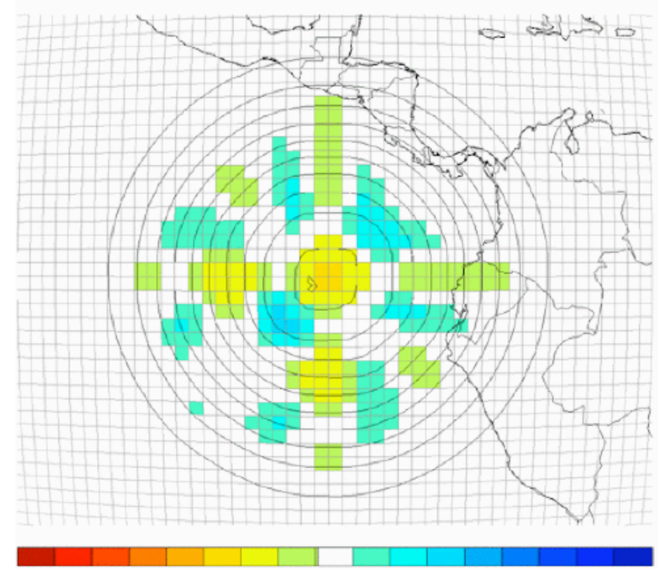

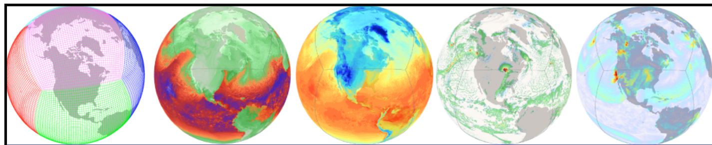

Finite-Volume Advection

general curvilinear coordinates

(Putman and Lin, 2007)

Contravariant Winds

$$\vec{V} = \tilde{u}\vec{e_1} + \tilde{v}\vec{e_2}$$

Covariant Winds

$$u = \vec{V} \cdot \vec{e_1}$$

$$v = \vec{V} \cdot \vec{e_2}$$

$$cos(\alpha) = \vec{e_1} \cdot \vec{e_2}$$

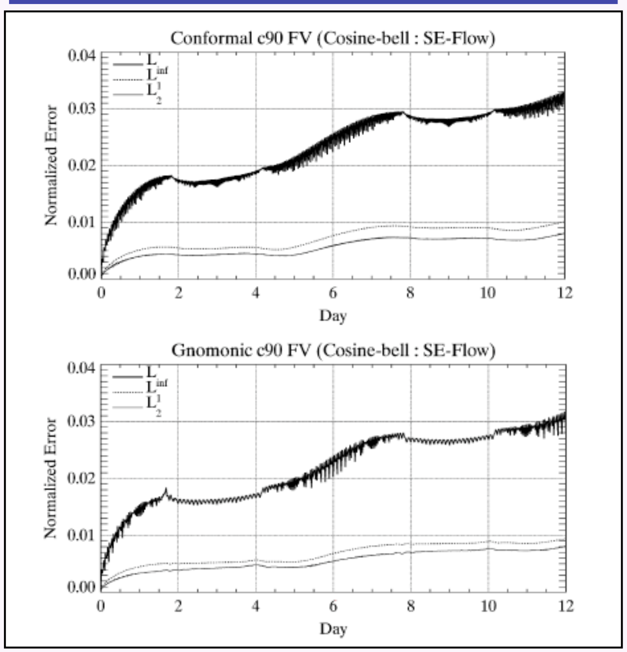

- Eulerian
- Stable for CFL < 1
- Adapted for non-orthogonal grids
- Allows use of Gnomonic grids

$$\tilde{\pi}^{n+1} = \tilde{\pi}^n + F\left[\widetilde{u^*}, \Delta t, \pi^y\right] + G\left[\widetilde{v^*}, \Delta t, \pi^x\right]$$

$$F(\widetilde{u^*}, \Delta t, \tilde{\pi}^n) = -\frac{\Delta t}{\Delta \mathcal{A}}\delta_x\left[\chi\, \Delta y\, sin(\alpha)\right]$$

$$= -\frac{\Delta t}{\Delta \mathcal{A}}\delta_x\left[\widetilde{u^*}\, \pi^*(\widetilde{u^*}, \Delta t, \tilde{\pi}^n)\, \Delta y\, sin(\alpha)\right]$$

$$G(\widetilde{v^*}, \Delta t, \tilde{\pi}^n) = -\frac{\Delta t}{\Delta \mathcal{A}}\delta_y\left[Y\, \Delta x\, sin(\alpha)\right]$$

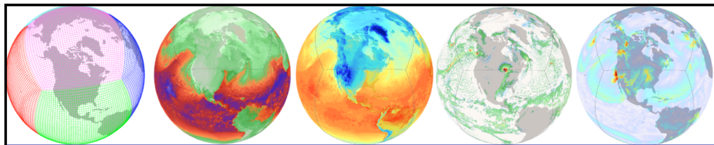

Finite-Volume Advection

Sub-Grid Distribution Schemes

- An optimized PPM (labeled ORD=4)
- A Quasi-monotonic scheme with Huynh's 2nd constraint (ORD=5)
- A non-monotonic quasi-5th order scheme (ORD=6)
- The ORD=5 scheme with explicit treatment for edge discontinuities on the cubed-sphere (ORD=7)

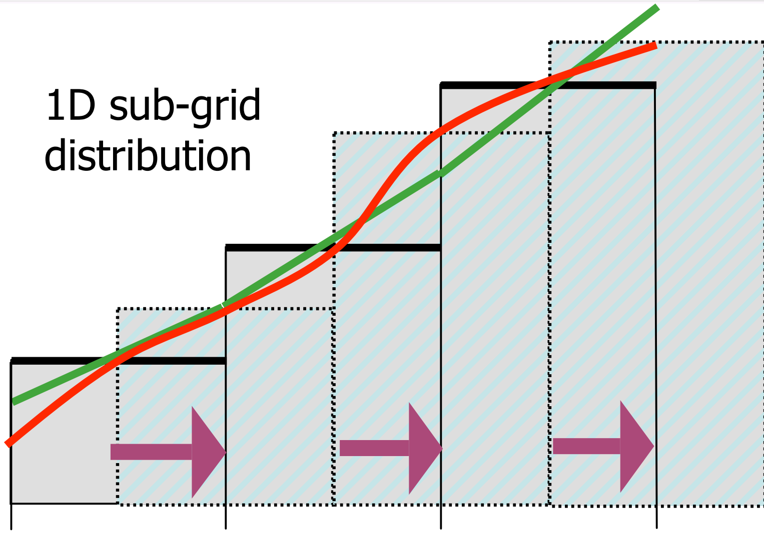

ORD=7 details (*4th order and continuous before monotonicity*)…

$$q_e = \frac{1}{2}\left[\frac{3}{2}(q_1^r + q_0^l) - \frac{1}{2}(q_2^r + q_{-1}^l)\right]$$

•The value at the edge is an average of two one-sided 2nd order extrapolations across edge discontinuities

$$q_e \leftarrow \max(0, q_e)$$

•Positivity for tracers

$$q_{e+}^r = \frac{1}{14}(3q_1^r + 11q_2^r - 2m_2^r)$$

•Fitting by Cubic Polynomial to find the value on the other edge of the cell
- vanishing 2nd derivative
- local mean = cell mean of left/right cells
- local slope consistent with orig PPM

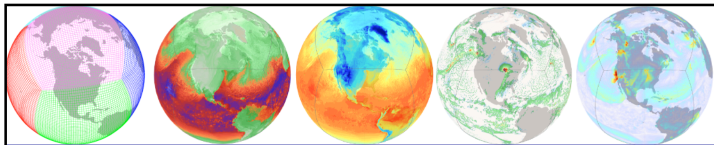

SCIENCE
MISSION DIRECTORATE

c180 geos_fv_cubed_dycore_2-0-1234_high_L26-hord4

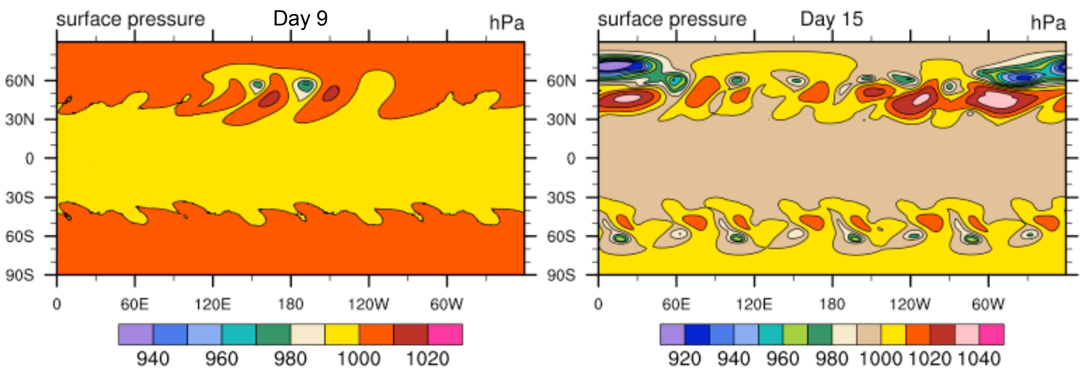

geos_fv_cubed_dycore_2-0-1234_high_L26-hord5

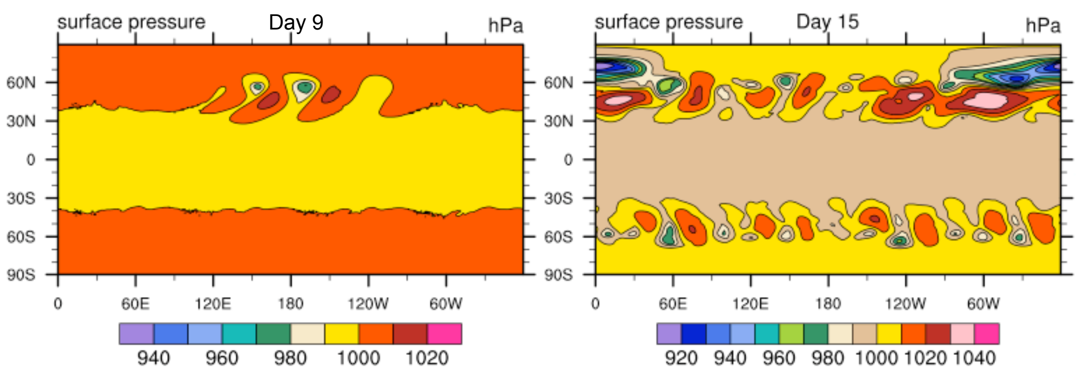

geos_fv_cubed_dycore_2-0-1234_high_L26-hord7

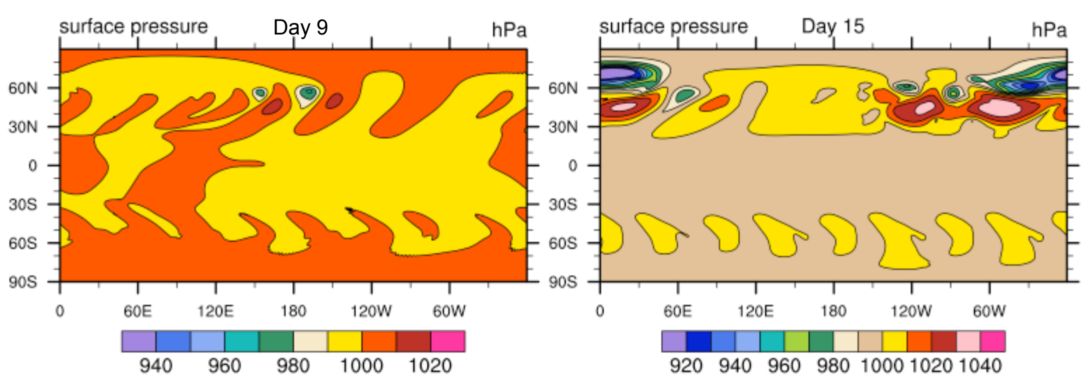

Jablonowski & Williamson Baroclinic Wave

- Impact of sub-grid distribution scheme on Surface Pressure evolution over 15-days
- hord=5 scheme requires small dt to be reduced from 75s to 45s
- Noticeably reduced wave-4 amplitude at day-15 with hord=7

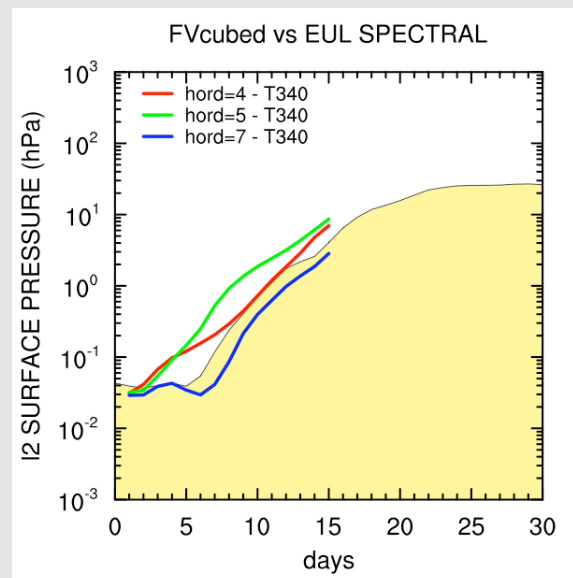

Finite-Volume Baroclinic Eqs

(From Lin 2004 MWR vol. 132)

Implicit Diffusion

Explicit Diffusion

$$\frac{\partial}{\partial t}\pi + \nabla \cdot (\mathbf{V}\pi) = 0 \qquad \frac{\partial}{\partial t}(\pi q) + \nabla \cdot (\mathbf{V}\pi q) = 0$$

Air Mass "pseudo-density"

$\pi = \partial p / \partial \zeta$

$$\frac{\partial}{\partial t}(\pi \Theta) + \nabla \cdot (\mathbf{V}\pi\Theta) = 0$$

$$\frac{\partial}{\partial t}u = \Omega v - \frac{1}{A\cos\theta}\left[\frac{\partial}{\partial \lambda}(\kappa + \phi - \nu D) + \frac{1}{\rho}\frac{\partial}{\partial \lambda}p)\right]$$

$$\frac{\partial}{\partial t}v = -\Omega u - \frac{1}{A}\left[\frac{\partial}{\partial \theta}(\kappa + \phi - \nu D) + \frac{1}{\rho}\frac{\partial}{\partial \theta}p\right]$$

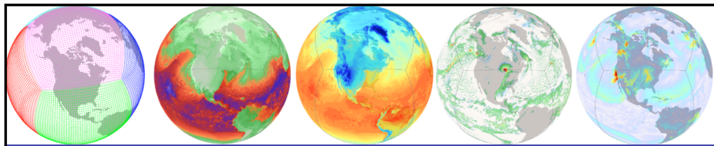

SCIENCE
MISSION DIRECTORATE

3D Gravity Wave Test

720x361 20L

Lat-Lon FV with default Divergence Damping

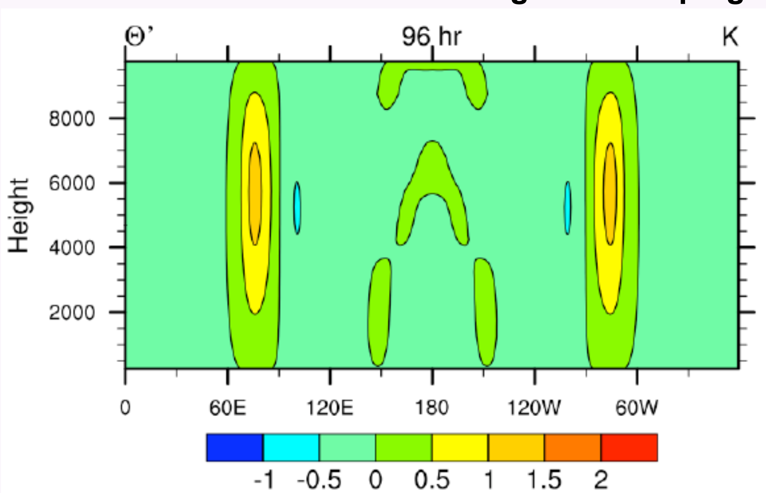

Cubed-Sphere FV with ∇^2 & ∇^4 Divergence Damping

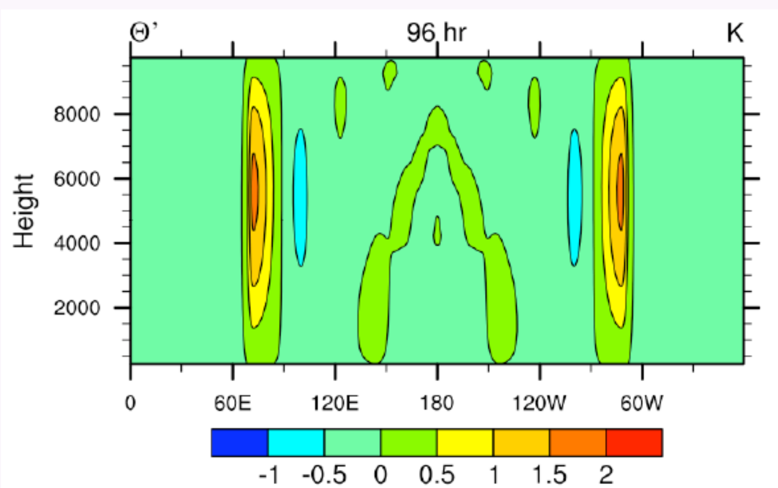

Horizontal Divergence Damping

- Original FV scheme had only ∇^2 divergence damping (2nd order)
- Cubed-Sphere FV scheme has introduced ∇^4, ∇^6, and ∇^8 divergence damping terms
- Reduced coefficient for ∇^2 term (can be 0.00)
- The impact is clear for gravity wave test case

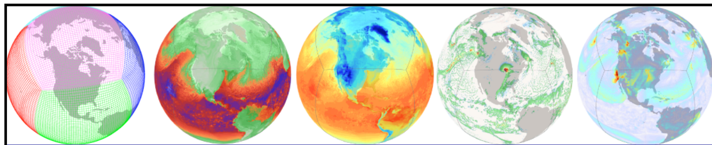

SCIENCE
MISSION DIRECTORATE

Horizontal Divergence Damping

geos_fv_dycore_2-0-1234_medium_high_L26

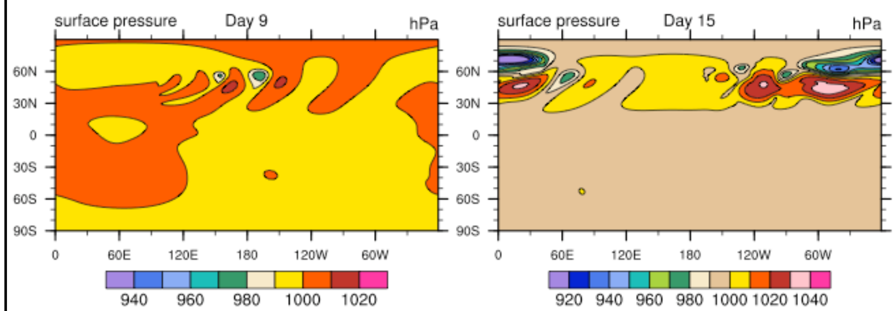

geos_fv_cubed_dycore_2-0-1234_medium_high_L26_del2-0.05

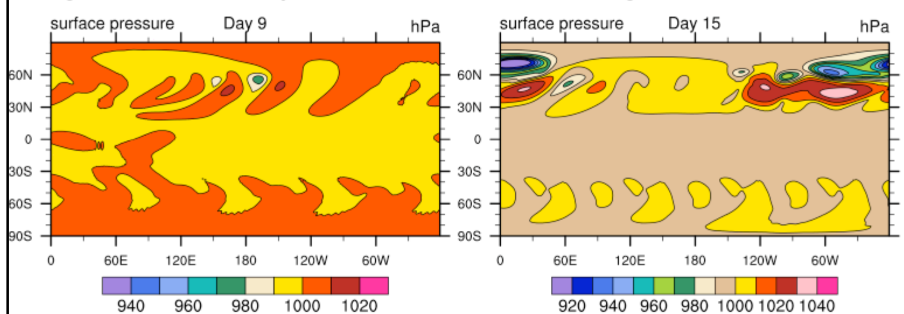

geos_fv_cubed_dycore_2-0-1234_medium_high_L26_del2-0.0_del4-0.2

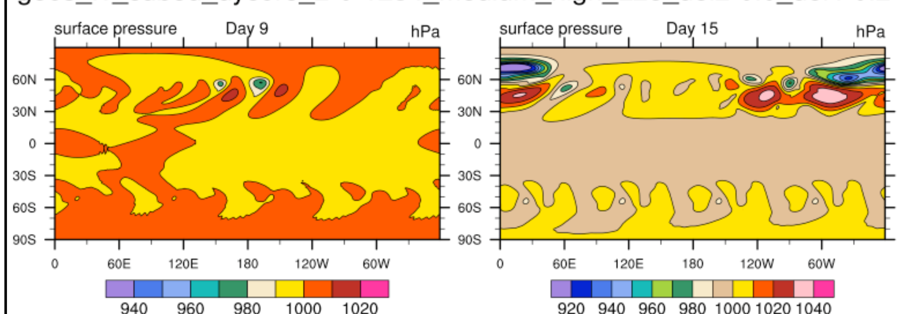

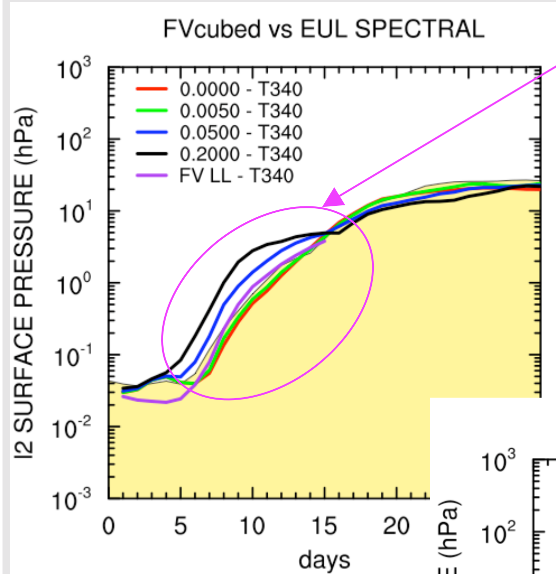

- ∇^2 divergence damping has a strong influence on the developing wave

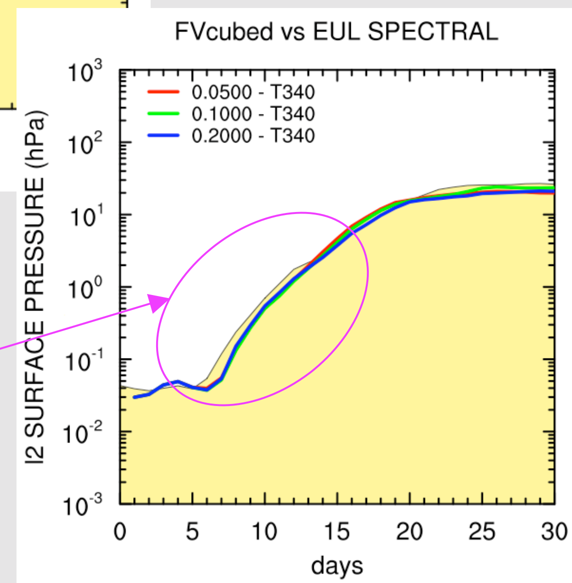

- ∇^4 divergence damping preserves the baroclinic wave structure

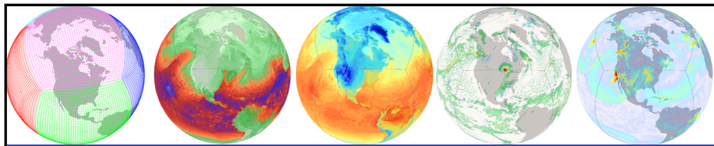

SCIENCE
MISSION DIRECTORATE

Kinetic Energy Spectra

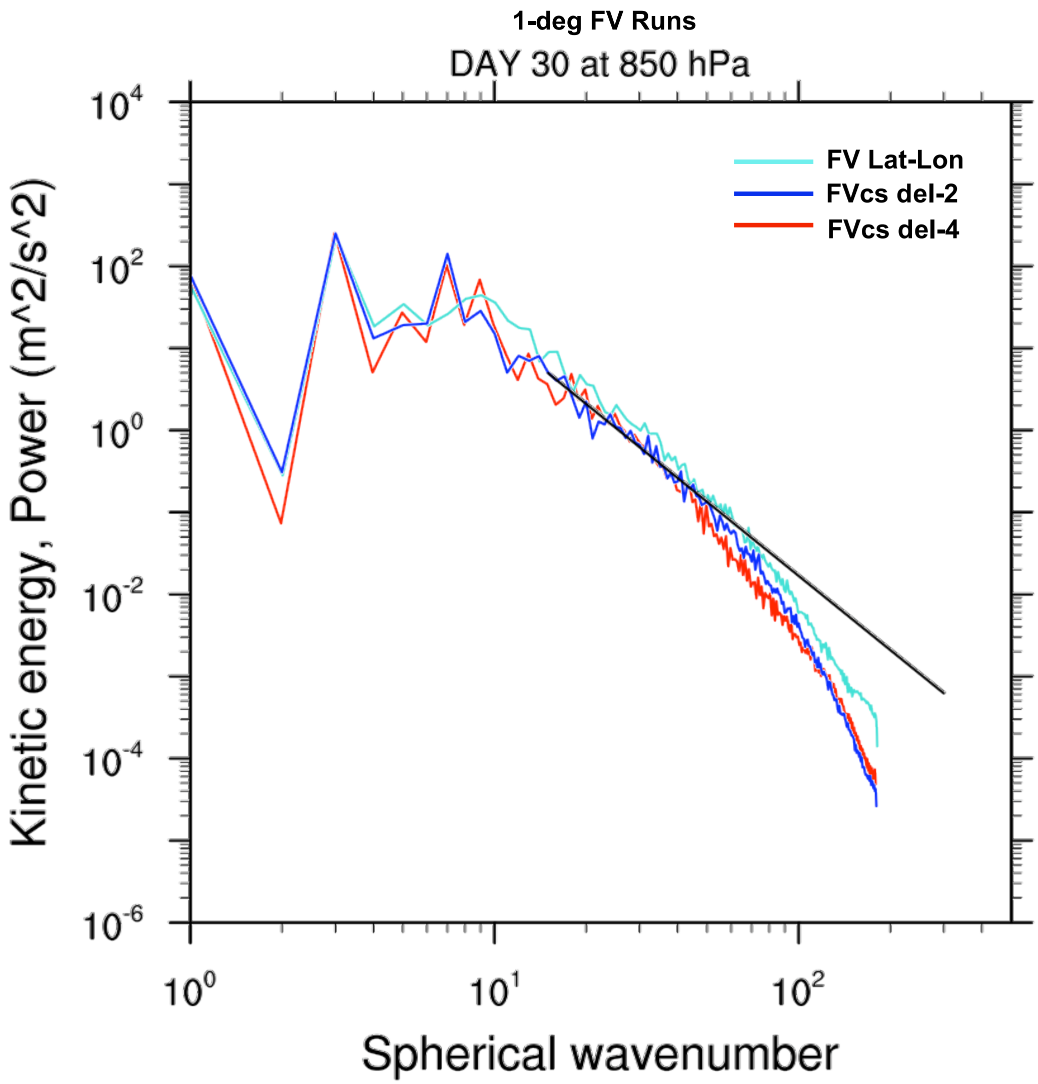

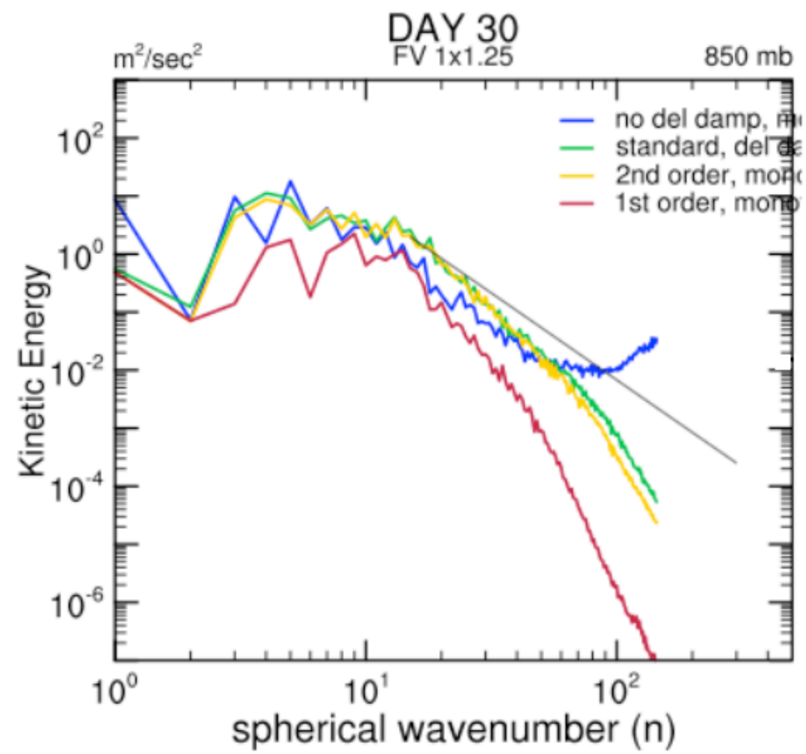

Credit: Jablonowski ASP Diffusion Talk

Grid Imprinting